Cell Tissue Res (2014) 358:807–819
DOI 10.1007/s00441-014-1993-7

REGULAR ARTICLE

Regional changes in elastic fiber organization and transforming growth factor β signaling in aortas from a mouse model of marfan syndrome

David W. Howell · Natasa Popovic · Richard P. Metz · Emily Wilson

Received: 29 April 2014 / Accepted: 21 August 2014 / Published online: 20 September 2014

Abstract In Marfan Syndrome (MFS), development of thoracic aortic aneurysms (TAAs) is characterized by degeneration of the medial layer of the aorta, including fragmentation and loss of elastic fibers, phenotypic changes in the smooth muscle cells, and an increase in the active form of transforming growth factor-β (TGFβ), which is thought to play a major role in development and progression of the aneurysm. We hypothesized that regional difference in elastic fiber fragmentation contributes to TGFβ activation and hence the localization of aneurysm formation. The fibrillin-1-deficient mgR/mgR mouse model of MFS was used to investigate regional changes in elastin fiber fragmentation, TGFβ activation and changes in gene expression as compared to wild-type littermates. Knockdown of Smad 2 and Smad 3 with shRNA was used to determine the role of the specific transcription factors in gene regulation in aortic smooth muscle cells. We show increased elastin fiber fragmentation in the regions associated with aneurysm formation and altered TGFβ signaling in these regions. Differential effects of Smad 2 and Smad 3 were observed in cultured smooth muscle cells by shRNA-mediated knockdown of expression of these transcription factors. Differential signaling through Smad 2 and Smad 3 in regions of active vascular remodeling likely contribute to aneurysm formation in the mgR/mgR model of MFS. Increased elastin fiber fragmentation in these regions is associated with these changes as compared to other regions of the thoracic aorta and may contribute to the changes in TGFβ signaling in these regions.

D. W. Howell · N. Popovic · R. P. Metz · E. Wilson (✉)
Department of Medical Physiology, Texas A&M Health Science Center, College Station, TX 77843-1114, USA
e-mail: ewilson@tamhsc.edu

Keywords Thoracic aortic aneurysm · Regional aortic changes · TGFβ · Elastin fiber fragmentation and Marfan mouse model

Introduction

A thoracic aortic aneurysm (TAA) is defined as a progressively expanding abnormal dilation of the thoracic region of the aorta resulting in increased weakening of the aorta. Rupture and dissection of an aneurysm are associated with a high degree of mortality, despite continued improvements in surgical techniques (Coady et al. 1999). Development of TAAs is characterized by degeneration of the medial layer of the aorta, including fragmentation and loss of elastic fibers and increased deposition of proteoglycans. Additionally, there are phenotypic changes in the smooth muscle cells and ultimately loss of cells from the vascular wall. These changes result in a thinning of the aortic wall coupled with an increase in the diameter of the aorta in these sites. Rupture of the aortic wall can lead to high mortality (LeMaire and Russell 2008; Milewicz, et al. 2008). Several genetic syndromes predispose individuals to the development of TAAs, the most prominent and best studied being Marfan syndrome (MFS) (Milewicz et al. 2008). Mutations in the Fibrillin-1 (FBN1) gene, a large microfibrillar glycoprotein found in the extracellular matrix that associates with elastin, are the cause of MFS (Francke et al. 1995; Katzke et al. 2002). Study of mouse models having reduced FBN1 expression have led to a better understanding of the molecular nature of MFS and associated TAA development (Dietz et al. 2005). In addition to alterations in the elastin-associated microfibrils, there is an increase in the active form of transforming growth factor-β (TGFβ) in humans (Habashi et al. 2006; Neptune et al. 2003) and in mouse models of MFS as compared to wild-type (WT) mice,

suggesting a critical role for TGFβ in the pathogenesis of TAAs (Neptune et al. 2003).

TGFβ is a multifunctional polypeptide growth factor involved in the regulation of cell growth and differentiation as well as immune functions (Massague 2000; Patterson and Padgett 2000; Ten Dijke et al. 2002). In the vasculature, TGFβ is an important regulator of balanced ECM deposition (Roberts et al. 1986) and degradation (Laiho et al. 1986; Selvamurugan et al. 2004). In the pathogenesis of TAAs, however, hyperactivation of TGFβ signaling leads to enhanced proteolysis of the vascular ECM (Jones et al. 2009) in conjunction with TGFβ-mediated SMC apoptosis (Fukui et al. 2003; Henderson et al. 1999; Sho et al. 2005) and fibroblast differentiation to myofibroblasts (Shi et al. 1996; Vaughan et al. 2000; Willis and Borok 2007). TGFβ mediates effects through ligand binding to a receptor that initiates signaling through phosphorylation of the Smad proteins (Shi and Massagué 2003). The Smad family of proteins can be divided into three functional groups: the receptor-activated Smads (R-Smads), common mediator Smads (Co-Smads), and the inhibitory Smads (I-Smads). The R-Smads are directly phosphorylated by the activated type I receptor and include Smad 1, Smad 2, Smad 3, Smad 5, and Smad 8. Smad 2 and Smad 3 are phosphorylated in response to TGFβ and activin. C-terminal phosphorylation of the R-Smads initiates binding to Co-Smads and translocation to the nucleus where they can recruit transcriptional co-regulators, which results in transcription of specific TGFβ target genes (Brown et al. 2007).

Although TGFβ activates both Smad 2 and Smad 3, it is now clear that these two proteins mediate different transcriptional responses in cells and play distinct roles in pathophysiologic effects of TGFβ (Roberts et al. 2003). Regulation of Smad 2 and Smad 3 is complex and can occur at the level of the TGFβ receptors, nuclear import and export, protein turnover, and/or the transcriptional level (Kurisaki et al. 2001; Lin et al. 2004; Nakao et al. 1997; Pierreux et al. 2000; Tsukazaki et al. 1998; Xiao et al. 2000; Xu et al. 2002). Recent data suggest that Smad 3 is the key mediator of pathogenic effects of TGFβ in fibrosis (Flanders 2004), but increased knowledge of the unique roles and distinct transcriptional targets of Smad 2 and Smad 3 is needed to determine the complex role of TGFβ in cells and tissues and the specific role of these regulators in the initiation and progression of TAAs.

We hypothesize that the regions of the thoracic aorta involved in TAAs exhibit altered TGFβ signaling compared with other areas of the aorta. This altered signaling may occur due to increased elastic fiber fragmentation in regions of high mechanical stress (Hodis and Zamir 2011), different embryonic origins of smooth muscle cells in the susceptible regions (Pietri et al. 2003), or a combination of these and other factors. To test this hypothesis, we explored spatial patterns of signaling through the TGFβ pathway, morphological characteristics of the aorta, and characteristics of elastic lamellae in the Fbn-1-deficient Fbn-$1^{mgR/mgR}$ mouse model of Marfan syndrome (referred to as mgR/mgR) (Pereira et al. 1999). Furthermore, we characterized regional expression of known TGFβ-regulated genes in aortas from mgR/mgR and WT mice and used differential knockdown of Smad 2 or Smad 3 in cultured vascular smooth muscle cells (VSMC) to determine their individual roles in gene expression.

Materials and methods

Animals and tissue isolation

Breeding pairs of mgR/mgR C57/S129 mice were obtained originally from Dr. Francesco Ramirez, Mount Sinai Hospital, NY, USA. Breeding pairs and their offspring were maintained and used in accordance with the University Laboratory Animal Care committee (ULACC) guidelines. Fifteen mgR/mgR and 15 age-matched WT mice between 8 and 14 weeks of age were used. Mice were anesthesized by IP injection of 50 mg/kg of sodium pentobarbital then exsanguinated. The aorta from the heart to the diaphragm was isolated, placed in a sterile saline solution, and cleaned from adventitial tissue and blood. For the protein and RNA isolations, each aorta was cut into 4 segments: section 0 from the heart to the brachiocephalic (ascending aorta), section 1 between brachiocephalic and left subclavian artery (aortic arch), section 2 (proximal half of descending aorta), and section 3 (distal part of descending aorta) (Fig. 1b). Segments were placed in 1.7-ml conical tubes, snap frozen in liquid nitrogen, and stored in the −80 °C freezer until further processing.

Cell culture

Thoracic aortic vascular smooth muscle cells explanted from WT mice were transfected (passage 5–10) with shRNA constructs using Genejuice (Merck-Millipore, Darmstadt, Germany) transfection reagent per manufacturer's instructions. The shRNA constructs were generated using the pSilencer puro kit (Life Technologies, Grand Island, NY, USA) and the following sequences to silence Smad 2 (5′GGATCCAAGAATTTGCTGCTCTTCTTTCAAGA GAAGAAGAGCAG CAAATTCTTGGTTTTTTGGAAA AGCTT -3′) and Smad 3 (5-GATCCAACGCAG AACG TGAACACCAAGTTCAAGAGACTTGGTGTTCACGT TCTGCGTGTTTTTTGGAAA-3′). Cells were then treated with 5 ng/ml TGFβ or vehicle for 24 h after serum starvation for 24 h.

Antibodies

Anti-pSMAD-2 (Cat #3108), anti-pSMAD 2/3 (Cat #3122), and anti-pSMAD-3 (Cat #8769) antibody was purchased from

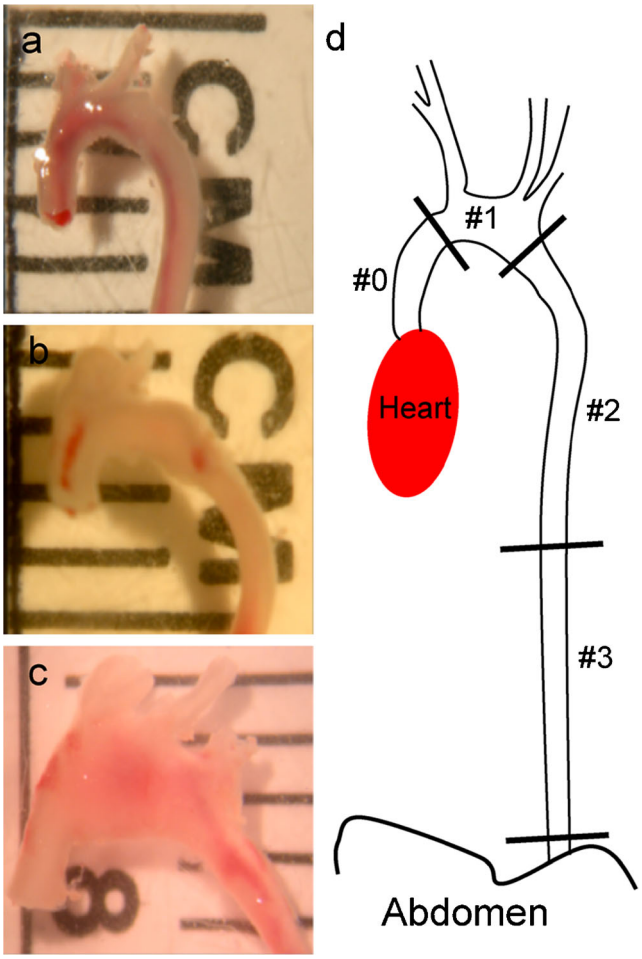

Fig. 1 Development and progression of TAA in aortas from the mgR/mgR mouse model. From left to right aortas were taken from **a** Wild-type mouse of 8 weeks and mgR/mgR mice of **b** 8 and **c** 15 weeks. **d** Tissue isolation schema. Each aorta was cut into 4 segments: section 0 from the heart to the brachiocephalic (ascending aorta), section 1 between brachiocephalic and left subclavian artery (aortic arch), section 2 (proximal half of descending aorta), and section 3 (distal part of descending aorta)

Cell Signaling Technology, Beverly, MA, USA. Anti-GAPDH (product code 2-RGM2) antibody was purchased from Advanced Immunochemical, Long Beach, CA, USA.

Western blot analysis

Frozen aortic sections from mgR/mgR mice were pulverized and lysed in ice-cold lysis buffer (20 mM Tris pH 7.4, 50 mM NaCl, 50 mM NaF, 50 mM EDTA, 20 mM Na pyrophosphate, 1 mM Na orthovanadate, 1 % TritonX-100 and protease inhibitor cocktail set 1 by Calbiochem, Gibbstown, NJ, USA (Cat #539131)). Protein lysates from each aortic section containing 15 mg of protein were precipitated by methanol and chloroform, and resuspended in 2× sample buffer (0.126 M Tris–HCl, pH=6.8, 12.6 % Glycerol, 0.004 % bromophenol blue, 5 % sodium dodecyl sulphate, and 1.44 M beta mercaptoethanol). The samples were subjected to SDS-polyacrylamide electrophoresis with MOPS running buffer (4-12 % Bis-Tris gradient gel; NuPAGE Novex) and transferred to nitrocellulose membranes. Protein molecular weight ranges were determined relative to SeeBlue Plus2 Pre-stained Standards (Invitrogen, Carlsbad, CA, USA). The membrane was cut right above the 39-kDa marker band and both pieces were blocked in 5 % nonfat dry milk in TTBS (1× TBS, pH 7.5, and 0.05 % Tween). The top half of the membrane was incubated with primary antibody (1:500) overnight at 4 °C; the bottom part was incubated with anti-GAPDH antibody (1:1000) for 1 h at 4 °C. Membranes were then incubated with the appropriate horseradish peroxidase-conjugated secondary antibody for 1 h at room temperature and visualized by incubation with Super Signal West Femto Maximum Sensitivity Substrate (Cat# 34095; Thermo Scientific, Waltham, MA, USA). Images were captured using a LAS-4000 Image Reader (FUJIFILM, USA). Quantification of western blots was performed using densitometric analysis functions of Image Studio Lite (LI-COR Biosciences, Lincoln, NE, USA).

Histology

Whole aortas isolated from 3 mgR/mgR mice and 3 age matched wild type controls were cleaned from adventitia and blood and fixed in 4 % paraformaldehyde overnight (approximately 16 h) at 4 °C, then transferred to 70 % ethanol and kept at 4 °C until further processing. Next, each segment was labeled with a different color of India ink: ascending aorta with green, arch with blue, proximal part of descending aorta with black and distal part of the descending aorta with orange. Ascending aorta and arch were specifically labeled at the outer curvature. Before embedding, aortas were cut into 4 segments that were positioned parallel to each other and embedded in a few-mm-thick layer of paraffin. The paraffin sheet was then embedded in a paraffin block, hence cross-sections of all four aortic segments could be cut and processed on the same slide and at the same time. Sections were further stained following Verhoef van Gieson (VVG) with hematoxylin and eosin (H&E) counter staining. Images were captured with an Olympus BX51 microscope with an Olympus DP70 camera with ×10 and ×40 objectives, and scored using a custom image analysis program as previously described (Hu et al. 2007).

RNA isolation and DNAse treatment

Frozen aortic segments were pulverized and total RNA was isolated by using TRIzol® Reagent (Cat #15596-026; Invitrogen, Carlsbad, CA, USA) by following manufacturer's instructions. DNAse treatment was used to remove any possible DNA contamination (DNA-free, Ambion, Austin, TX, USA). RNA quantity, purity, and integrity was assessed by an Agilent 2100 Bioanalyzer (Agilent Technologies, Santa Clara, CA, USA).

RT-PCR

Sets of primers for mouse (Table 1) were designed and reverse transcription and real-time RT-PCR reactions were performed. Expression levels were calculated by using the delta Ct method, and normalized to the expression of the GAPDH for that particular sample. In order to compare results among different plates, results from the each plate were further normalized to the calibrator (DNA standard used to compare reactions between plates).

Statistical analysis

Data were analyzed by univariate analysis of variance (ANOVA) with independent sample *t* test in SPSS statistical software and post-ANOVA contrasts for planned comparisons in R Project software (R Development Core Team, 2008).

Results

Cross-sectional area and wall thickness of ascending aorta and arch are increased in mgR/mgR mice

Development and progression of aneurysms are located in the ascending aorta and aortic arch in our mgR/mgR mouse model (Fig. 1a–c). For analysis of regional changes, tissue was isolated from the thoracic aorta and divided into 4 segments as illustrated in Fig. 1d. Analysis of VVG stained cross-sections of aorta from the 4 different locations (Fig. 2a–h) showed that the wall thickness is higher in mgR/mgR than WT mice in the segment 0, the ascending aorta (111.01 vs. 95.41 μm, $P=0.008$; Fig. 2a, e, i). As expected, there is a trend of decreasing wall thickness in segments located more distally from the heart (mean wall thickness of mgR/mgR mice in the ascending aorta 111.01 vs. 85.68 μm in distal part of descending aorta, $P<0.001$; Fig. 2a–i). Next, the analysis showed that the cross-sectional areas ($2\pi rh$, r=radius, h=wall thickness) of the ascending aorta and arch are significantly larger relative to other aortic segments in mgR/mgR mice, and any segment of age-matched wild-type controls (1.57 vs. 1.25 mm^2 for segment 0, 2.33 vs. 1.37 mm^2 for segment 1, $P=0.01$; Fig. 2a–h, j). Interestingly, the ratio of radius to wall thickness is increased in the aortic arch regardless of genotype (Fig. 2k).

mgR/mgR mice show increased degradation of elastic lamina

VVG stained aortic cross-sections showed significant destruction of elastic lamina compared to WT control mice (Fig. 3a–h). The thickness of elastic lamina and elastin content are decreased in mgR/mgR mice ($P<0.001$,Fig. 3i, j) in all segments compared to WT. In addition, interlamellar distance is increased in mgR/mgR mice compared to the WT mice in all segments. Interlamellar distance analysis also showed that elastic laminae are packed more densely in the areas of the aorta closer to the heart ($P<0.001$; Fig. 3k).

Aberrant aortic morphology associates with increased phosphorylation of Smad 3

We previously observed increases of Smad 3 phosphorylation with age, and this increase is exaggerated in mgR/mgR mice having tortuous aorta (Popovic, unpublished observation). We speculated that the level of Smad 3 signaling might be related to the tortuosity. To explore that possibility, that there is differential phosphorylation of Smad 2 and 3 in regions of active aneurysm formation, we performed western blot analysis on 4 segments of aorta in 3 mgR/mgR mice at 15 weeks of age using an antibody that recognized both pSmad 2 and 3 (Fig. 4a). All 3 mice had aneurysms involving the arch and ascending aorta. One mouse had especially aberrant aortic morphology (Mouse 2, Fig. 4c). The upper band in the pSmad blot was prominent in all 4 regions and there was no statistical difference between regions (Fig. 4b). This band was confirmed to be pSmad 2. The lower band was confirmed to be pSmad 3 and was only observed in regions of active aneurysm formation (e.g. segments 0 and 1) and extreme aberrant morphology (Mouse 2) (Fig. 4b). Mouse 2 had gross morphological changes including severe dilation of the whole TA, an aneurysm that includes both segments 1 and 2 and increased tortuosity of segments 2 and 3. No increases in pSmad 3 were observed in WT mice in these same regions.

Regional differences in expression of TGFβ-regulated genes in aneurysm prone mice

Aortic segments of mgR/mgR mice and age-matched WT littermates were analyzed using RT-PCR to better determine the spatial changes in gene expression of aneurysm prone mice (mgR/mgR). For this study, we focused on a panel of smooth muscle contractile genes, extracellular matrix-associated genes, and signaling molecules that had been previously shown to be regulated by TGFβ signaling. Table 1 shows genes that were determined to be altered in segment 1 (aortic arch) of the mgR/mgR mice compared to WT littermates. Detailed analysis of several representative genes showed regional changes in expression (Fig. 5). Expression of collagen I in mgR/mgR mice is higher in the aortic arch than in WT littermates (4.02 vs. 3.5, $P=0.01$; Fig. 5a). SnoN expression in mgR/mgR mice is lower in the ascending aorta and aortic arch than in WT littermates (3.9 vs. 5.6 for segment 0 and 3.7 vs. 4.26 for segment 1, $P=0.01$; Fig. 5b). Expression of PAI-1 in mgR/mgR mice is higher in the aortic arch than in WT littermates (10.26 vs. 7.89, $P=0.01$; Fig. 5c).

Table 1 Representative TGFβ-modulated genes that are altered in segment 1 of aorta

Genes	Abbr.	Function	Primer sequence
Genes upregulated in segment 1 of mgR/mgR compared to wild-type			
Contractile genes			
Smooth muscle actin alpha 2	Acta2	Found in muscle tissues and are a major constituent of the contractile apparatus.	F: 5′ – ACG AAC GCT TCC GCT GC – 3′ R: 5′ – GAT GCC CGC TGA CTC CAT – 3′
Smooth muscle actin gamma 2	Actg2	Component of the cytoskeleton that acts as a mediator of internal cell motility.	F: 5′ – GCC CTG GAT TTC GAG AAT GA – 3′ R: 5′ – CCA TCA GGC AAC TCG TAG CTT – 3′
ECM genes			
Elastin	ELN	A connective tissue protein that allows tissue to resume shape after stretching or contracting.	F: 5′ – CTG GTG GTG TTA CTG GTA TTG GA – 3′ R: 5′ – GCC TTA GCA GCA GAT TTA GCG – 3′
Pro-collagen 1	Procol1	Fibril-forming collagen found in most connective tissues abundant in bone, cornea, dermis and tendon.	F: 5′ – CCC CGG GAC TCC TGG ACT T – 3′ R: 5′ – GCT CCG ACA CGC CCT CTC TC – 3′
Pro-collagen 3	Procol3	Collagen found in granulation tissue, and is produced quickly by young fibroblasts before the tougher type I collagen is synthesized.	F: 5′ – TTC CTG AAG ATG TCG TTG ATG TG – 3′ R: 5′ –TTT TTG CAG TGG TAT GTA ATG TTC TG -3′
Signaling genes			
Angiotensin II receptor, type 1a	Agtr1a	Responsible for the signal transduction of the vasoconstricting stimulus of the main effector hormone, angiotensin II.	F: 5′ –CAA GCC TGT CTA CGA AAA TGA G– 3′ R: 5′ –AAG ACG CAG GCT TTT TGG CG– 3′
Chymase 2, mast cell	Cma2	A serine protease found primarily in mast cells promoting an inflammatory response. Chymases are also known to convert angiotensin I to angiotensin II and thus play a role in hypertension and atherosclerosis.	F: 5′ –GAC GCG GAA ATG CAA AGC– 3′ R: 5′ –TCT GTT AAT CCA GGG CAC ATG T– 3′
Forkhead box P3	Foxp3	A member of the FOX protein family, FOXP3 appears to function as a master regulator in the development and function of regulatory T cells.	F: 5′ – CCC ACC TAC AGG CCC TTC TC– 3′ R: 5′ – GGC ATG GGC ATC CAC AGT – 3′
Plasminogen activator Inhibitor-1	PAI-1	Inhibitor of fibrinolysis.	F: 5′ – GGC ACA GTG GCG TCT TCC T – 3′ R: 5′ – TGC CGA ACC ACA AAG AGA AAG – 3′
SMAD mothers against DPP homolog 7	Smad 7	Inhibitory Smad	F: 5′ –CAG CAC TGC CAA GCA TGG T– 3′ R: 5′ –GCA CGG ACA ACC GAA ACG– 3′
Zinc finger protein SNAI1	Snail	Snail participates in the TGFβ signaling pathway upstream of Akt.	F: 5′ – CAC CCT CAT CTG GGA CTC TC – 3′ R: 5′ – CTT CAC ATC CGA GTG GGT TT – 3′
Genes downregulated in segment 1 of mgR/mgR compared to wild-type			
Contractile genes			
Myosin 11	MYH11	The myosin superfamily is a large class of motor molecules that interact with actin filaments to generate force or exert movement using energy generated through ATP hydrolysis	F: 5′ –AGC TGT TCA ACC ACA CGA TGT T– 3′ R: 5′ –GTT CGG CCG CTC AAT CAG G– 3′
Signaling genes			
Insulin-like growth factor	IGF1	Mainly secreted by the liver as a result of stimulation by growth hormone (GH). IGF-1 is important for both the regulation of normal physiology and changes in a number of pathological states. The IGF axis has been shown to play roles in the promotion of cell proliferation and the inhibition of cell death (apoptosis).	F: 5′ –GCT CCG GAA GCA ACA CTC AT– 3′ R: 5′ –GCT ATG GCT CCA GCA TTC G– 3′
Insulin-like growth factor-binding protein 3	IGFbp3	This protein forms a ternary complex with insulin-like growth factor acid-labile subunit (IGFALS) and	F: 5′ – CAC ACC GAG TGA CCG ATT – 3′ R: 5′ – GGC CTT TTT TGA TGA CAT CCA – 3′

Table 1 (continued)

Genes	Abbr.	Function	Primer sequence
		either insulin-like growth factor (IGF) I or II. In this form, it circulates in the plasma, prolonging the half-life of IGFs and altering their interaction with cell surface receptors.	
Insulin-like growth factor 1 receptor	IGFr1	A transmembrane receptor that is activated by Insulin-like growth factor 1 and 2.	F: 5′ – AGC GCA GCT GAT GTG TAC GT – 3′ R: 5′ – TCC GAG CTC CCG GTT CA – 3′
SKI-like oncogene	SnoN	Negative regulator of TGFβ signaling. Binds to nuclear Smad complexes, repressing transcriptional activities.	F: 5′ – ATA CAC CAT CGG GAA TGG AA – 3′ R: 5′ – CAT GAT CTT CCC CTT GTC GT – 3′
E3 ubiquitin-protein ligase SMURF1	Smurf1	A ubiquitin ligase that is specific for receptor-regulated SMAD proteins	F: 5′ –CGG GAG TGG CTG TAT TTG TT– 3′ R: 5′ –GTG CTA AGA ACT GGG CTT CG – 3′

Differential contributions of Smad 2 and 3 in TGFβ-mediated gene expression

To determine if there is differential contribution of Smad 2 and Smad 3 to TGFβ-mediated gene expression in mouse thoracic aortic smooth muscle cells, an shRNA knockdown approach was used. Aortic smooth muscle cell lines were made in which expression of either Smad 2 or Smad 3 was constitutively decreased by infection with lentiviral vectors containing the shRNAs (Fig. 6a) and were used to explore the role of Smad 2 and Smad 3 in TGFβ-induced expression of Collagen 1, SnoN and PAI-1. Expression of Collagen 1 in Smad 2-specific shRNA-treated VSMCs is lower when treated with TGFβ (Fig. 6b). Expression of Collagen I in Smad 3-specific shRNA-treated VSMCs is unchanged (Fig. 6c), suggesting that TGFβ predominantly signals through Smad 2 to alter expression of collagen 1. Expression of SnoN in Smad 2-specific shRNA-treated VSMCs is lower when treated with TGFβ (Fig. 6d), while expression of SnoN in Smad 3-specific shRNA-treated VSMCs is unchanged (Fig. 6e), suggesting that TGFβ predominantly signals through Smad 2 to alter expression of SnoN. Expression of PAI-1 in Smad 3-specific shRNA-treated VSMCs is lower when treated with TGFβ (Fig. 6f), while expression of PAI-1 in Smad 2-specific shRNA-treated VSMCs is unchanged (Fig. 6g), suggesting that TGFβ predominantly signals through Smad 3 to alter expression of PAI-1.

Discussion

Dissection of TAAs is associated with high mortality and, while better diagnostic tools and surgical methods have both prolonged life and improved the quality of life of those suffering from TAA, increased knowledge of the molecular mechanism leading to aneurysm formation and dissection may identify better targets for treatment (Coady et al. 1999). In genetic models of TAA, such as MFS, the mutation is found throughout the body and hence the genetic changes are observed all along the aorta, yet aneurysms only form in the ascending and arch region of the aorta. Two hypotheses have emerged as to the basis for the location of TAAs. The first hypothesis considers the unique mechanical environment of the ascending aorta and arch region to be a major contributor to the location of aneurysm formation (Hodis and Zamir 2011), and the second is that the origin of the smooth muscle cells in this region (i.e. neural crest and second heart field) contribute to the location (Pietri et al. 2003). In the current study, we used the mgR/mgR mouse model of MFS to detail regional changes of structural changes in the aorta, TGFβ signaling, and gene expression for their potential contribution to aneurysm growth. The mgR/mgR mouse model was used previously to identify the role of TGFβ in TAA formation and is a well-characterized mouse model of MFS (Pereira et al. 1999).

The structure of the aortic wall is critical for keeping wall stress within physiologic values (Humphrey 2008). This structure depends on the distance from the heart as well as the presence of curvatures and branches (Sherwood 2008). In agreement with this, we confirm that elastic laminae are more densely packed in regions closer to the heart and wall thickness decreases in regions that are more distant from the heart (Fig. 2a–k). In particular, the arch has the highest radius to wall thickness in both genotypes, which underlines the fact that wall structure in this region is unique (Fig. 2k). In addition, we observed the high density of elastin lamellas and the highest wall thickness in the area of ascending aorta and arch, which emphasizes the importance of elastin and vessel compliance in this area for optimal function (Fig. 3a–k). Therefore, it appears that effects of elastin fragmentation on wall stiffness become apparent first in this region and this early change may contribute both to TGFβ activation and aneurysm development in this region.

In Fbn-1-deficient mice, macroscopic appearance of the vessel wall in the area of the arch and ascending aorta, and

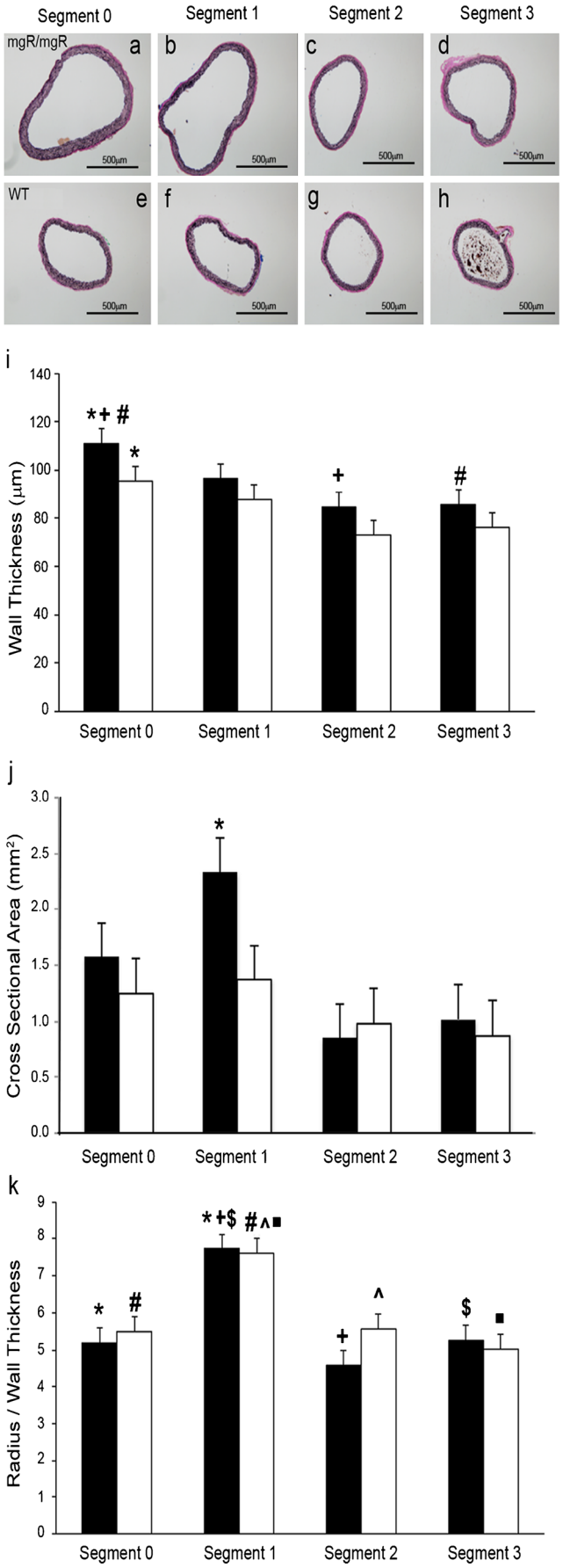

Fig. 2 Cross-sectional area and wall thickness of ascending aorta and arch are increased in mgR/mgR mice. **a–h** Representative VVG stained cross-sections of 4 aortic segments of 12-week-old mgR/mgR mouse (*top*) and age-matched wild-type (WT) control (*bottom*) at ×100 magnification. **i** Wall thickness is higher in the ascending aorta of mgR/mgR (*black bars*) compared to wild type (*white bars*) mice ($P=0.008$), and it decreases with increased distance from the heart ($P<0.001$). Statistically significant relationships are denoted by matching symbols: *, +, and #. *Error bars* standard error of the mean (SEM), ($n=6$). **j** Cross-sectional area of the arch of mgR/mgR (*black bars*) mice is larger relative to other segments in mgR/mgR mice as well as any segment in age matched WT controls (*white bars*) ($P<0.001$). T*Denotes that segment 1 of mgR/mgR is statistically significant compared to all other segments of both mgR/mgR and WT. *Error bars* SEM, ($n=6$). **k** Ratio of radius to wall thickness is higher in aortic arch regardless of genotype ($P<0.001$). Statistically significant relationships are denoted by matching symbols: *, +, $, ^, ■ and #. *Error bars* SEM, ($n=6$)

sometimes even major aortic branches, is strikingly different from the rest of the aorta (Fig. 1a–c). We hypothesized that this is related to the unique shape of this region, extreme spatial and temporal variability of wall stresses, and inadequate remodeling inherent to this disorder. However, the fact that most of the cardiac outflow tract (ascending aorta, arch and major branches excluding left subclavian artery) has neuroectodermal embryonic origin should be taken into account as well (Pietri et al. 2003). It has been shown that TGFβ1 inhibits differentiation of SMC of mesenchymal origin in cell culture, while it has the opposite effect on neuroectoderm-derived SMC (Topouzis and Majesky 1996).

Our data suggest a role for increased Smad3 activity in the areas where there is active aneurysm development (Fig. 4) as indicated by increased pSmad 3 in the ascending aorta and arch segments. Mutations in Smad 3 have also been reported in families that develop TAAs, thus supporting a role for Smad 3 in aneurysm development (van de Laar et al. 2011). Our observations do not rule out other downstream signaling pathways such as the non-canonical activation of members of the Mitogen activated protein kinase (MAPK) family (Holm et al. 2011). Our data simply support a role for Smad 3 in the overall process.

In agreement with our observation, recently published studies provide an argument for increased signaling through the TGFβ pathway as a direct cause for development of aortic aneurysms. Namely, Habashi and colleagues demonstrated that multiple organ abnormalities associated with Marfan syndrome are caused by increased activation of TGFβ (Habashi et al. 2006). Fatini and colleagues showed further that angiotensin converting enzyme polymorphism ACE I/D is associated with higher incidence of abdominal aortic aneurysms, and they speculated this is probably due to increased expression of angiotensin convertase, resulting in increased signaling though the TGFβ pathway (Fatini et al. 2005). Our observation agrees with studies arguing that increased signaling through the TGFβ pathway may be a consequence of changes in aortic compliance associated with elastin

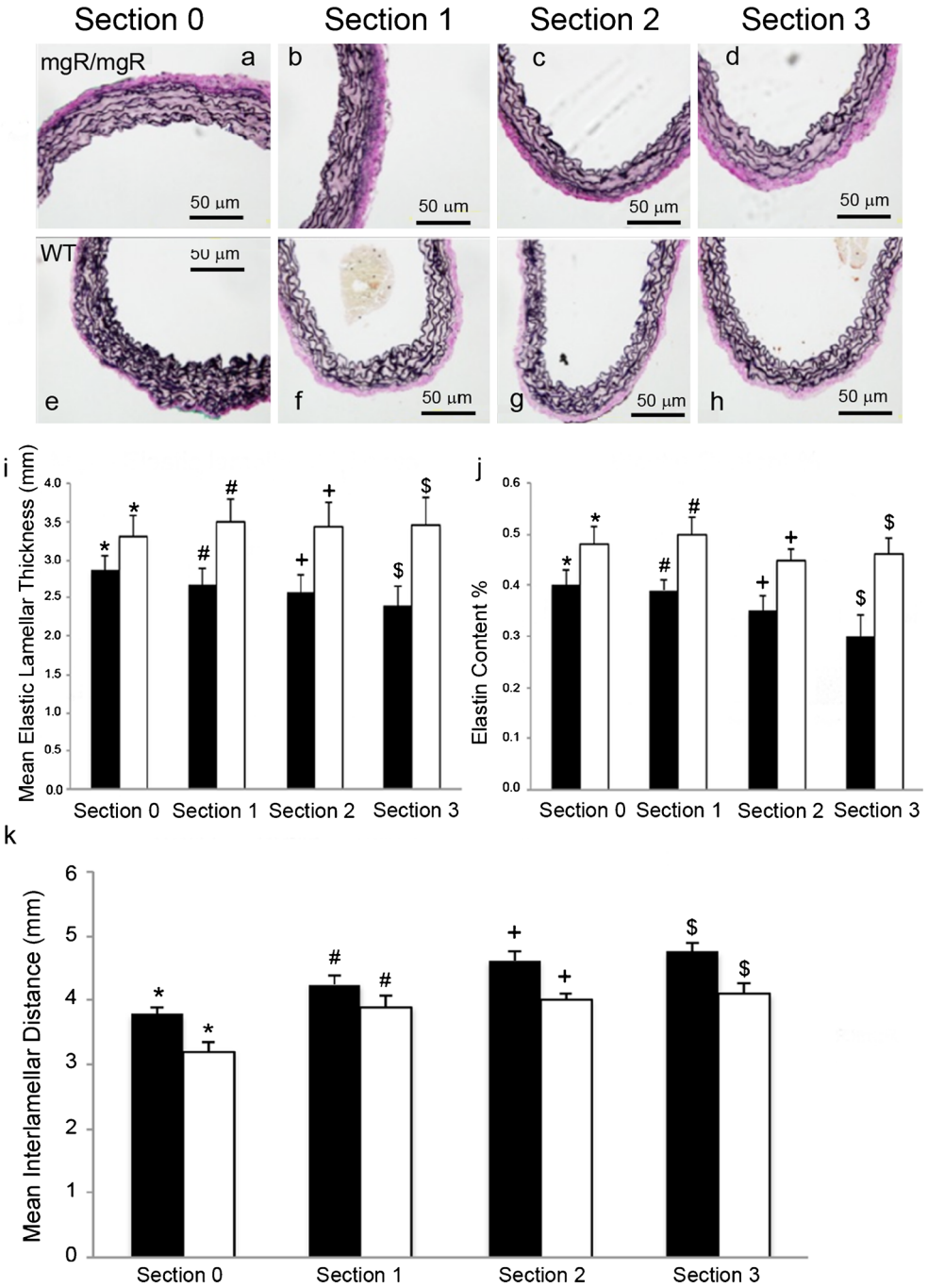

Fig. 3 mgR/mgR mice show increased degradation of elastic laminae. Representative VVG stained cross-sections of 4 aortic segments of 12-week-old mgR/mgR mouse (*top*, **a**–**d**) and age-matched wild-type (WT) control (*bottom*, **e**–**h**) at ×40 magnification. Note significant fragmentation of elastic lamina in mgR/mgR relative to the age-matched WT control mouse. **i** Elastic laminae thickness and **j** elastin content expressed as % of total tissue (*right*) are decreased in mgR/mgR mice (*black bars*) compared to WT (*white bars*) mice ($P<0.001$ for both graphs). Statistically significant increase between mgR/mgR and WT in section 0 is denoted by *, in section 1 by #, in section 2 by +, and in section 3 by $. **k** Interlamellar distance is higher in mgR/mgR mice (*black bars*) compared to WT (*white bars*) controls ($P<0.001$). Interlamellar distance is lower in areas closer to the heart ($P=0.028$). *Error bars* standard error of the mean, ($n=6$). Statistically significant decrease between mgR/mgR and WT in section 0 is denoted by *, in section 1 by #, in section 2 by +, and in section 3 by $

fragmentation and development of the aneurysm, since we observed increased elastin fragmentation and decreased size of the elastic lamina in the regions where aneurysms form. Although we did not measure compliance or stiffness directly, the increased elastin fragmentation would be associated with changes in compliance. For example, Wipff and others demonstrated that TGFβ activation and signaling through Smad 2/3 is higher if myofibroblasts are cultured in stiff ECM. (Wipff et al. 2007)

To further characterize the mgR/mgR mutation and its link to altered TGFβ signaling through Smad 2/3 we used RT-PCR analysis to examine expression of known TGFβ-regulated genes regionally in aortas. Multiple genes, including contractile genes, extracellular matrix, and signaling molecules, were tested (Table 1), and many showed a significant difference in expression in the segments where aneurysms form. These data suggest that alteration in a number of genes contribute to development and progression of TAAs. Among the genes that are upregulated are the smooth muscle actin genes, ACTA2 and ACTG2. These genes are associated with the differentiation status of smooth muscle and mutations in ACTA2 have been identified in some patients with familial TAAs (Guo et al.

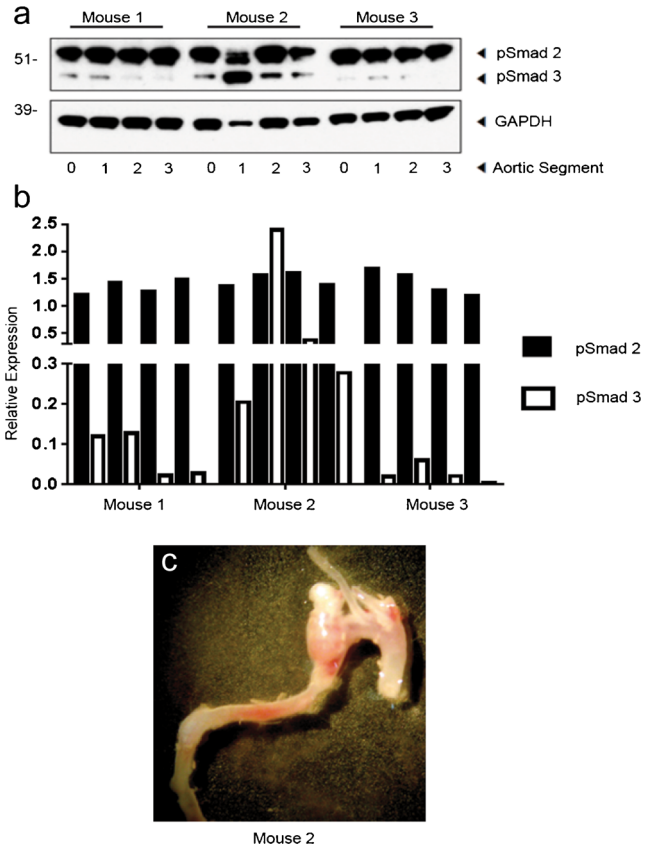

Fig. 4 Aberrant aortic morphology associates with increased phosphorylation of Smad 3. **a** Western blot of protein lysates isolated from 4 aortic segments of 3 mice with large aneurysms involving ascending aorta and arch (average age 12 weeks). Note the pattern of higher expression of Smad 3 in the arch area. **b** Quantification of western blot in Fig. 4a for pSmad 2 and pSmad 3 normalized to GAPDH. The *upper band* in the blot, confirmed to be pSmad 2, was prominent in all 4 regions and there was no statistical differences between regions. The lower band was confirmed to be pSmad 3 and was only observed in regions of active aneurysm formation (e.g., segments 0 and 1) and extreme aberrant morphology (Mouse 2). **c** Photograph of whole-mount mouse aorta isolated form 12-week-old animal with aberrant morphology in the ascending aorta and aortic arch, which are strikingly different from the rest of the aorta

2009). Additionally, mRNAs for the extracellular matrix proteins elastin, collagen 1 and collagen 3 are upregulated suggesting reorganization of the ECM in this region, and there is increased expression of plasminogen activator inhibitor-1 (PAI-1), a regulator of protease activity that is involved in ECM degradation. Interestingly, genes associated with angiotensin signaling, including the angiotensin II 1a receptor and chymase, were upregulated. Blockade of the Ang II receptor with Losartan is now being used as a therapy in TAA (Cook et al. 2010; Habashi et al. 2006). Several modifiers of TGFβ signaling, including Smad 7 and Snail, were upregulated. Among the genes that showed decreased expression were components of the insulin-like growth factor pathway including IGF1, IGF 1 receptor and IGF1 binding protein 3. IGF signaling contributes to survival of smooth muscle and

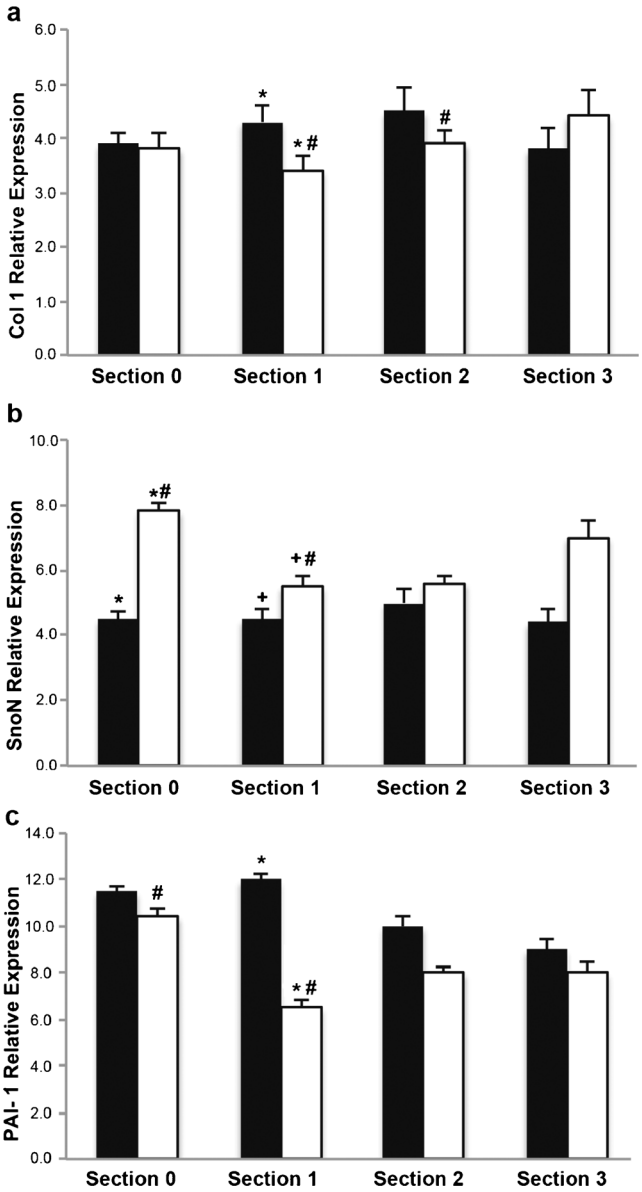

Fig. 5 Regional changes in representative TGFβ–regulated genes in thoracic aorta of mgR/mgR and wild-type (WT) mice. **a** Graphical representation of qRT-PCR results for relative expression of Collagen I in mgR/mgR mice (*black bars*) is lower in the aortic arch than in WT littermates (*white bars*) (P=0.01). *Error bars* standard error of the mean (SEM), (n=15). The statistically significant decrease of mgR/mgR compared to WT is denoted by * and the significant increase between section 1 and 2 in mgR/mgR mice is denoted by #. **b** Graphical representation of qRT-PCR results for relative expression of SnoN in mgR/mgR (*black bars*) mice is lower in the ascending aorta and arch than in WT littermates (*white bars*) (p=0.01). *Error bars* standard error of the mean (SEM), (n=15). The statistically significant increase of mgR/mgR compared to WT in section 0 is denoted by * and by + in section 1. The significant decrease between section 0 and 1 in mgR/mgR mice is denoted by #. **c** Graphical representation of qRT-PCR results for relative expression of PAI-1 in mgR/mgR (*black bars*) mice is lower in the aortic arch than in WT littermates (*white bars*) (p=0.01). *Error bars* SEM, (n=15). The statistically significant decrease of mgR/mgR compared to WT in section 1 is denoted by *. The significant decrease between section 0 and 1 in mgR/mgR mice is denoted by #

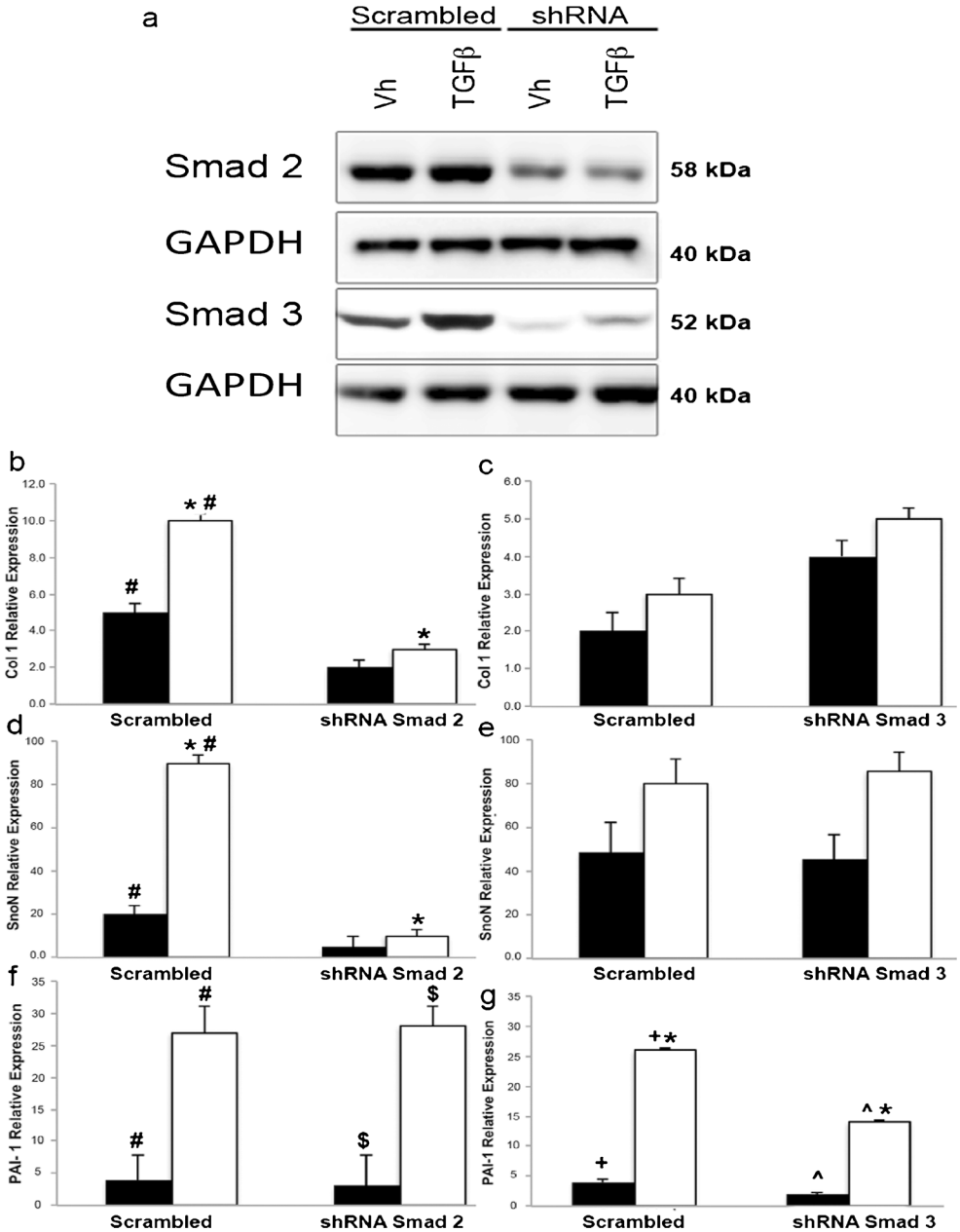

Fig. 6 shRNA knockdown of Smad 2 and Smad 3 reveal differential effects on TGFβ-medicated gene expression in vascular smooth muscle cells (VSMC). **a** Western blot shows knockdown of Smad 2 and Smad 3 using shRNA in VSMC. **b** Expression of collagen I in Smad 2-specific shRNA-treated VSMCs is lower in the TGFβ-treated group (*white bar*) when compared to the scrambled control (P=0.001, indicated by *). Under normal conditions (scrambled, *white* vs. *black bars*), TGFβ increases expression of collagen I (P=0.01, indicated by #). **c** Expression of collagen I in Smad 3-specific shRNA-treated VSMCs shows no significant difference between scrambled and shRNA-treated VSMCs in the untreated control group (*black bar*) or TGFβ group (*white bar*). *Error bars* standard error of the mean (SEM), (n=3). **d** Expression of SnoN in Smad 2-specific shRNA-treated VSMCs is lower when treated with TGFβ (*white bar*, significance of P=0.001 is denoted by *). Under normal conditions (scrambled, *white* vs. *black bars*), TGFβ increases expression of SnoN (P=0.01, indicated by #). **e** Expression of SnoN in Smad 3-specific shRNA-treated VSMCs is unchanged when treated with TGFβ (*white bar*) or in the vehicle control group (*black bar*). *Error bars* SEM, (n=3). **f** Expression of PAI-1 in Smad 2-specific shRNA-treated and scrambled control VSMCs is increased when treated with TGFβ (*white* vs. *black bars*, P=0.001, indicated by # in scrambled and $ in shRNA-treated cells). **g** Expression of PAI-1 in Smad 3-specific shRNA-treated VSMCs is lower than scrambled when treated with TGFβ (*white bar*, significance of P=0.001 is denoted by *). However, TGFβ does increase PAI-1 expression compared to vehicle in both scrambled (P=0.005, denoted by +) and Smad 3-specific shRNA-treated VSMCs (P=0.01, denoted by ^). *Error bars* SEM, (n=3). There is no significant difference between scrambled and shRNA-treated VSMCs in the vehicle control group (*black bar*)

decreased expression in this region may contribute to the loss of smooth muscle cells during aneurysm development (Allen, et al., 2005). Additionally, there is decreased expression of SnoN, a repressor of Smad signaling, and Smurf, a ubiquitin

ligase that is specific for Smad proteins. Decreased expression of these genes would be expected to contribute to increased signaling through Smad 2/3 pathway (Doyle 2012). Recent studies have shown that mutations in SnoN are associated with TAA formation in Shprintzen-Goldberg syndrome (Doyle 2012). Thus, a number of genes may contribute to the vascular remodeling in these regions associated with aneurysm formation. Detailed expression profiles of three of the significant genes are shown in Fig. 5 for illustration and because of their potential mechanistic role in aneurysm formation and progression. The differences in the expression profiles indicated that some changes may be directly linked to the changes in FBN1 expression and that others are related to the location in the aorta suggesting that both of these factors contribute to the site of aneurysm formation.

Collagen is the core component of fibrous collagenous tissues (Fratzl 2008), whose organization into suprafibrillar structures are a key component of gradual remodeling and weakening of the aneurysm wall (Choke et al. 2005) due to the strong structural aspect of fibrillar collagens in the tissue (He and Roach 1994; Macsweeney et al. 1992). During TAA progression elastin fragmentation leads to a weakening of the vascular wall while collagen content increases in order to maintain homeostasis (Fig. 5a) (Rizzo et al. 1989). TGFβ is a potent inducer of ECM protein synthesis and accumulation, implicating it as a mediator of fibrosis (Border and Noble 1994; Pohlers et al. 2009). It has been shown that TGFβ modulates collagen type 1 (Col 1) through the Smad pathway (Derynck and Zhang 2003; Poncelet et al. 1999; Tsukada et al. 2005). To determine if there were differential effects of Smad 2 or Smad 3 on Col 1 expression in aortic smooth muscle, we used a lentiviral system and shRNA to specifically decrease expression levels of either Smad 2 or Smad 3. The cells with diminished Smad 2 expression showed decreased Col1 expression in response to TGFβ, whereas there was no effect on TGFβ-induced expression when Smad 3 was diminished. These data are consistent with Smad 2 transcriptional regulation being the predominant mechanism for TGFβ-induced Col 1 mRNA expression in aortic smooth muscle (Fig. 6b, c).

SnoN is a TGFβ signaling repressor that sequesters Smad proteins in the cytoplasm and prevents their phosphorylation and translocation into the nucleus. SnoN inhibition of TGFβ signaling is especially potent in conditions with prolonged stimulation of cells by this growth factor such as would be seen in regions of aneurysm formation. To determine which of the Smads are involved in this process, we again used the shRNA system described above to determine which of the two Smads potentially contribute to altered SnoN mRNA expression. Both basal and TGFβ-induced expression were decreased in the Smad 2 deficient cells and there was no effect on either in the Smad 3 deficient cells. These data suggest that both basal expression and TGFβ-mediated increases in transcription of SnoN (Stroschein, et al., 1999) are through Smad 2 and not Smad 3 signaling (Fig. 6d, e). It is possible that this form of inhibition occurs in the aged aortic SMCs that are exposed to increased stimulation by TGFβ for a long time. Moreover, signals transmitted through pSmad 2 and pSmad 3 are unequally affected by SnoN in the nucleus (Stroschein et al. 1999). Transcription of genes targeted by pSmad 2 is repressed by SnoN, but, in the presence of pSmad 3, the half-life and nuclear abundance of SnoN decreases, and transcription of TGFβ target genes is upregulated (Stroschein et al. 1999). This is supported by our data showing that expression of SnoN is lower in mgR/mgR mice (Fig. 5b) possibly due to higher Smad 3 signaling.

PAI-1 is the major physiologic regulator of the plasmin-based pericellular proteolytic cascade, which modulates vascular smooth muscle cell migration leading to tissue fibrosis and cardiovascular disease (Agirbasli 2005; Bhoday et al. 2006; Degryse et al. 2004; DeYoung et al. 2001; Eddy and Fogo 2006; Kohler and Grant 2000; Sobel et al. 2003; Vaughan 2002). We confirm that there is an increased expression of PAI-1 mRNA in areas of aneurysm formation in the mgR/mgR model (Fig. 5c). We show that TGFβ-induced PAI-1 mRNA is not effected when Smad 2 is altered through shRNA knockdown but is when Smad 3 is altered, suggesting a Smad 3-dependant pathway in cultured aortic smooth muscle (Fig. 6f and g). This is consistent with other cell types as previously reported (Dennler et al. 1998; Stroschein; 1999).

Taken together, these data show that aberrant blood vessel morphology in the mgR/mgR model of Marfan syndrome develops most frequently at the locations known to have extremely variable blood flow and wall stresses—in the ascending aorta and aortic arch. Signaling through both Smad 2 and Smad 3 likely contribute to changes in gene expression associated with aneurysm formation. In addition, we show that altered TGFβ signaling through Smad 2/3 spatially associates with these areas and that the altered TGFβ signaling could account for much of the pathological change in the characterization of the vascular wall. More research is needed to determine the specific relationship between factors such as changes in TGFβ signaling patterns, including altered stoichiometry of Smad 2 and Smad 3 phosphorylation, unique properties of wall stresses and blood flow in this area, and increased wall stiffness due to elastin degradation.

Acknowledgements We thank Erin Ashmore for excellent advice and assistance with all aspects of the laboratory, Christina Thiel for technical help with experiments, Dr. Jay Humphrey for critical reading of the manuscript and suggestions throughout the study and Dr. Jerome Trzeciakowski for suggestions regarding statistical analysis. Dr. Metz is now associated with Texas AgriLife Genomics and Bioinformatics Services, Bourlaug Center College Station, TX.

Grants This research was supported by NIH grant R21 EB004106 (EW) and HL-092380 (EW).

Disclosures None.

References

Agirbasli M (2005) Pivotal role of plasminogen-activator inhibitor 1 in vascular disease. Int J Clin Pract 59:102–106

Allen RT, Krueger KD, Dhume A, Agrawal DK (2005) Sustained Akt/PKB activation and transient attenuation of c-jun N-Terminal kinase in the inhibition of apoptosis by IGF-1 in vascular smooth muscle cells. Apoptosis 10:525–535

Bhoday J, de Silva S, Xu Q (2006) The molecular mechanisms of vascular restenosis: Which genes are crucial? Curr Vasc Pharmacol 4:269–275

Border WA, Noble NA (1994) Transforming Growth Factor β in Tissue Fibrosis. N Engl J Med 331:1286–1292

Brown KA, Pietenpol JA, Moses HL (2007) A tale of two proteins: Differential roles and regulation of Smad2 and Smad3 in TGF-β signaling. J Cell Biochem 101:9–33

Choke E, Cockerill G, Wilson WRW, Sayed S, Dawson J, Loftus I, Thompson MM (2005) A Review of Biological Factors Implicated in Abdominal Aortic Aneurysm Rupture. Eur J Vasc Endovasc Surg 30:227–244

Coady MA, Rizzo JA, Goldstein LJ, Elefteriades JA (1999) Natural history, pathogenesis, and etiology of thoracic aortic aneurysms and dissections. Cardiol Clin 17:615–635

Cook JR, Nistala H, Ramirez F (2010) Drug-based therapies for vascular disease in Marfan syndrome: from mouse models to human patients. Mt Sinai J Med 77:366–373

Degryse B, Neels JG, Czekay R-P, Aertgeerts K, Y-i K, Loskutoff DJ (2004) The Low Density Lipoprotein Receptor-related Protein Is a Motogenic Receptor for Plasminogen Activator Inhibitor-1. J Biol Chem 279:22595–22604

Dennler S, Itoh S, Vivien D, ten Dijke P, Huet S, Gauthier JM (1998) Direct binding of Smad3 and Smad4 to critical TGFβ-inducible elements in the promoter of human plasminogen activator inhibitor-type 1 gene. EMBO J 17:3091–3100

Derynck R, Zhang YE (2003) Smad-dependent and Smad-independent pathways in TGF-[beta] family signalling. Nature 425:577–584

DeYoung MB, Tom C, Dichek DA (2001) Plasminogen Activator Inhibitor Type 1 Increases Neointima Formation in Balloon-Injured Rat Carotid Arteries. Circulation 104:1972–1971

Dietz HC, Loeys B, Carta L, Ramirez F (2005) Recent progress towards a molecular understanding of Marfan syndrome. Am J Med Genet C: Semin Med Genet 139C:4–9

Doyle AJ, Doyle JJ, Bessling SL, Maragh S, Lindsay ME, Schepers D, Gillis E, Mortier G, Homfray T, Sauls K, Norris RA, Huso ND, Leahy D, Mohr DW, Caulfield MJ, Scott AF, Destrée A, Hennekam RC, Arn PH, Curry CJ, Van Laer L, McCallion AS, Loeys BL, Dietz HC (2012) Mutations in the TGF-β repressor SKI cause Shprintzen-Goldberg syndrome with aortic aneurysm. Nat Genet 44:1249–1254

Eddy AA, Fogo AB (2006) Plasminogen Activator Inhibitor-1 in Chronic Kidney Disease: Evidence and Mechanisms of Action. J Am Soc Nephrol 17:2999–3012

Fatini C, Pratesi G, Sofi F, Gensini F, Sticchi E, Lari B, Pulli R, Dorigo W, Azas L, Pratesi C, Gensini GF, Abbate R (2005) ACE DD Genotype: A Predisposing Factor for Abdominal Aortic Aneurysm. Eur J Vasc Endovasc Surg 29:227–232

Flanders KC (2004) Smad3 as a mediator of the fibrotic response. Int J Exp Pathol 85:47–64

Francke U, Berg MA, Tynan K, Brenn T, Liu W, Aoyama T, Gasner C, Miller DC, Furthmayr H (1995) A Gly1127Ser mutation in an EGF-like domain of the fibrillin-1 gene is a risk factor for ascending aortic aneurysm and dissection. Am J Hum Genet 56:1287–1296

Fratzl P (2008) Collagen: Structure and Mechanics, an Introduction. In: Fratzl P (ed) Collagen. Springer, New York, pp 1–13

Fukui D, Miyagawa S, Soeda J, Tanaka K, Urayama H, Kawasaki S (2003) Overexpression of transforming growth factor β1 in smooth muscle cells of human abdominal aortic aneurysm. Eur J Vasc Endovasc Surg 25:540–545

Guo DC, Papke CL, Tran-Fadulu V, Regalado ES, Avidan N, Johnson RJ, Kim DH, Pannu H, Willing MC, Sparks E, Pyeritz RE, Singh MN, Dalman RL, Grotta JC, Marian AJ, Boerwinkle EA, Frazier LQ, LeMaire SA, Coselli JS, Estrera AL, Safi HJ, Veeraraghavan S, Muzny DM, Wheeler DA, Willerson JT, Yu RK, Shete SS, Scherer SE, Raman CS, Buja LM, Milewicz DM (2009) Mutations in Smooth Muscle Alpha-Actin (ACTA2) Cause Coronary Artery Disease, Stroke, and Moyamoya Disease, Along with Thoracic Aortic Disease. Am J Hum Genet 84:617–627

Habashi JP, Judge DP, Holm TM, Cohn RD, Loeys BL, Cooper TK, Myers L, Klein EC, Liu G, Calvi C, Podowski M, Neptune ER, Halushka MK, Bedja D, Gabrielson K, Rifkin DB, Carta L, Ramirez F, Huso DL, Dietz HC (2006) Losartan, an AT1 Antagonist, Prevents Aortic Aneurysm in a Mouse Model of Marfan Syndrome. Science 312:117–121

He CM, Roach MR (1994) The composition and mechanical properties of abdominal aortic aneurysms. J Vasc Surg 20:6–13

Henderson EL, Geng Y-J, Sukhova GK, Whittemore AD, Knox J, Libby P (1999) Death of Smooth Muscle Cells and Expression of Mediators of Apoptosis by T Lymphocytes in Human Abdominal Aortic Aneurysms. Circulation 99:96–104

Hodis S, Zamir M (2011) Mechanical events within the arterial wall under the forces of pulsatile flow: A review. J Mech Behav Biomed Mater 4:1595–1602

Holm TM, Habashi JP, Doyle JJ, Bedja D, Chen Y, van Erp C, Lindsay ME, Kim D, Schoenhoff F, Cohn RD, Loeys BL, Thomas CJ, Patnaik S, Marugan JJ, Judge DP, Dietz HC (2011) Noncanonical TGFβ Signaling Contributes to Aortic Aneurysm Progression in Marfan Syndrome Mice. Science 332:358–361

Hu JJ, Fossum TW, Miller MW, Xu H, Liu JC, Humphrey JD (2007) Biomechanics of the Porcine Basilar Artery in Hypertension. Ann Biomed Eng 35:19–29

Humphrey JD (2008) Mechanisms of Arterial Remodeling in Hypertension: Coupled Roles of Wall Shear and Intramural Stress. Hypertension 52:195–200

Jones JA, Spinale FG, Ikonomidis JS (2009) Transforming Growth Factor-β Signaling in Thoracic Aortic Aneurysm Development: A Paradox in Pathogenesis. J Vasc Res 46:119–137

Katzke S, Booms P, Tiecke F, Palz M, Pletschacher A, Türkmen S, Neumann LM, Pregla R, Leitner C, Schramm C, Lorenz P, Hagemeier C, Fuchs J, Skovby F, Rosenberg T, Robinson PN (2002) TGGE screening of the entire FBN1 coding sequence in 126 individuals with marfan syndrome and related fibrillinopathies. Hum Mutat 20:197–208

Kohler HP, Grant PJ (2000) Plasminogen-Activator Inhibitor Type 1 and Coronary Artery Disease. N Engl J Med 342:1792–1801

Kurisaki A, Kose S, Yoneda Y, Heldin C-H, Moustakas A (2001) Transforming Growth Factor-β Induces Nuclear Import of Smad3 in an Importin-β1 and Ran-dependent Manner. Mol Biol Cell 12:1079–1091

Laiho M, Saksela O, Keski-Oja J (1986) Transforming growth factor β alters plasminogen activator activity in human skin fibroblasts. Exp Cell Res 164:399–407

LeMaire SA, Russell L (2011) Epidemiology of thoracic aortic dissection. Nat Rev Cardiol 8:103–113

Lin H-K, Bergmann S, Pandolfi PP (2004) Cytoplasmic PML function in TGF-[beta] signalling. Nature 431:205–211

Macsweeney STR, Young G, Greenhalgh RM, Powell JT (1992) Mechanical properties of the aneurysmal aorta. Br J Surg 79:1281–1284

Massague J (2000) How cells read TGF-[beta] signals. Nat Rev Mol Cell Biol 1:169–178

Milewicz DM, Guo D-C, Tran-Fadulu V, Lafont AL, Papke CL, Inamoto S, Kwartler CS, Pannu H (2008) Genetic Basis of Thoracic Aortic

Aneurysms and Dissections: Focus on Smooth Muscle Cell Contractile Dysfunction. Annu Rev Genomics Hum Genet 9:283–302

Nakao A, Imamura T, Souchelnytskyi S, Kawabata M, Ishisaki A, Oeda E, Tamaki K, Ji H, Heldin CH, Miyazono K, ten Dijke P (1997) TGF-β receptor-mediated signalling through Smad2, Smad3 and Smad4. EMBO J 16:5353–5362

Neptune ER, Frischmeyer PA, Arking DE, Myers L, Bunton TE, Gayraud B, Ramirez F, Sakai LY, Dietz HC (2003) Dysregulation of TGF-[beta] activation contributes to pathogenesis in Marfan syndrome. Nat Genet 33:407–411

Patterson GI, Padgett RW (2000) TGFβ-related pathways: roles in Caenorhabditis elegans development. Trends Genet 16:27–33

Pereira L, Lee SY, Gayraud B, Andrikopoulos K, Shapiro SD, Bunton T, Biery NJ, Dietz HC, Sakai LY, Ramirez F (1999) Pathogenetic sequence for aneurysm revealed in mice underexpressing fibrillin-1. Proc Natl Acad Sci USA 96:3819–3823

Pierreux CE, Nicolás FJ, Hill CS (2000) Transforming Growth Factor β-Independent Shuttling of Smad4 between the Cytoplasm and Nucleus. Mol Cell Biol 20:9041–9054

Pietri T, Eder O, Blanche M, Thiery JP, Dufour S (2003) The human tissue plasminogen activator-Cre mouse: a new tool for targeting specifically neural crest cells and their derivatives in vivo. Dev Biol 259:176–187

Pohlers D, Brenmoehl J, Löffler I, Müller CK, Leipner C, Schultze-Mosgau S, Stallmach A, Kinne RW, Wolf G (2009) TGF-β and fibrosis in different organs — molecular pathway imprints. Biochim Biophys Acta (BBA) - Mol Basis Dis 1792:746–756

Poncelet A-C, De Caestecker MP, Schnaper HW (1999) The transforming growth factor-[bgr]/SMAD signaling pathway is present and functional in human mesangial cells. Kidney Int 56:1354–1365

R Development Core Team. (2008). R: A language and environment for statistical computing.R Foundation for Statistical Computing, Vienna, Austria. ISBN 3-900051-07-0, http://www.R-project.org

Rizzo RJ, McCarthy WJ, Dixit SN, Lilly MP, Shively VP, Flinn WR, Yao JST (1989) Collagen types and matrix protein content in human abdominal aortic aneurysms. J Vasc Surg 10:365–373

Roberts AB, Sporn MB, Assoian RK, Smith JM, Roche NS, Wakefield LM, Heine UI, Liotta LA, Falanga V, Kehrl JH (1986) Transforming growth factor type beta: rapid induction of fibrosis and angiogenesis in vivo and stimulation of collagen formation in vitro. Proc Natl Acad Sci USA 83:4167–4171

Roberts AB, Russo A, Felici A, Flanders KC (2003) Smad3: A Key Player in Pathogenetic Mechanisms Dependent on TGF-β. Ann N Y Acad Sci 995:1–10

Selvamurugan N, Kwok S, Alliston T, Reiss M, Partridge NC (2004) Transforming Growth Factor-β1 Regulation of Collagenase-3 Expression in Osteoblastic Cells by Cross-talk between the Smad and MAPK Signaling Pathways and Their Components, Smad2 and Runx2. J Biol Chem 279:19327–19334

Sherwood L (2008) Human Physiology: From Cells to Systems. Cengage Learning, Brooks/Cole

Shi Y, Massagué J (2003) Mechanisms of TGF-β Signaling from Cell Membrane to the Nucleus. Cell 113:685–700

Shi Y, O'Brien JE, Fard A, Zalewski A (1996) Transforming Growth Factor-β1 Expression and Myofibroblast Formation During Arterial Repair. Arterioscler Thromb Vasc Biol 16:1298–1305

Sho E, Sho M, Nanjo H, Kawamura K, Masuda H, Dalman RL (2005) Comparison of cell-type-specific vs transmural aortic gene expression in experimental aneurysms. J Vasc Surg 41:844–852

Sobel BE, Taatjes DJ, Schneider DJ (2003) Intramural Plasminogen Activator Inhibitor Type-1 and Coronary Atherosclerosis. Arterioscler Thromb Vasc Biol 23:1979–1989

Stroschein SL, Wang W, Luo K (1999) Cooperative Binding of Smad Proteins to Two Adjacent DNA Elements in the Plasminogen Activator Inhibitor-1 Promoter Mediates Transforming Growth Factor β-induced Smad-dependent Transcriptional Activation. J Biol Chem 274:9431–9441

Ten Dijke P, Goumans M-J, Itoh F, Itoh S (2002) Regulation of cell proliferation by Smad proteins. J Cell Physiol 191:1–16

Topouzis S, Majesky MW (1996) Smooth Muscle Lineage Diversity in the Chick Embryo: Two Types of Aortic Smooth Muscle Cell Differ in Growth and Receptor-Mediated Transcriptional Responses to Transforming Growth Factor-β. Dev Biol 178:430–445

Tsukada S, Westwick JK, Ikejima K, Sato N, Rippe RA (2005) SMAD and p38 MAPK Signaling Pathways Independently Regulate α1(I) Collagen Gene Expression in Unstimulated and Transforming Growth Factor-β-stimulated Hepatic Stellate Cells. J Biol Chem 280:10055–10064

Tsukazaki T, Chiang TA, Davison AF, Attisano L, Wrana JL (1998) SARA, a FYVE Domain Protein that Recruits Smad2 to the TGFβ Receptor. Cell 95:779–791

van de Laar IMBH, Oldenburg RA, Pals G, Roos-Hesselink JW, de Graaf BM, Verhagen JMA, Hoedemaekers YM, Willemsen R, Severijnen L-A, Venselaar H, Vriend G, Pattynama PM, Collee M, Majoor-Krakauer D, Poldermans D, Frohn-Mulder IME, Micha D, Timmermans J, Hilhorst-Hofstee Y, Bierma-Zeinstra SM, Willems PJ, Kros JM, Oei EHG, Oostra BA, Wessels MW, Bertoli-Avella AM (2011) Mutations in SMAD3 cause a syndromic form of aortic aneurysms and dissections with early-onset osteoarthritis. Nat Genet 43:121–126

Vaughan DE (2002) PAI-1 and Cellular Migration: Dabbling in Paradox. Arterioscler Thromb Vasc Biol 22:1522–1523

Vaughan MB, Howard EW, Tomasek JJ (2000) Transforming Growth Factor-β1 Promotes the Morphological and Functional Differentiation of the Myofibroblast. Exp Cell Res 257:180–189

Willis BC, Borok Z (2007) TGF-β-induced EMT: mechanisms and implications for fibrotic lung disease. Am J Physiol Lung Cell Mol Physiol 293:L525–L534

Wipff P-J, Rifkin DB, Meister J-J, Hinz B (2007) Myofibroblast contraction activates latent TGF-β1 from the extracellular matrix. J Cell Biol 179:1311–1323

Xiao Z, Liu X, Lodish HF (2000) Importin ß mediates nuclear translocation of Smad 3. J Biol Chem 275:23425–23428

Xu L, Kang Y, Çöl S, Massagué J (2002) Smad2 Nucleocytoplasmic Shuttling by Nucleoporins CAN/Nup214 and Nup153 Feeds TGFβ Signaling Complexes in the Cytoplasm and Nucleus. Mol Cell 10: 271–282